■ 6321

Extremum Seeking Control for Power Output Maximization of Proton Exchange Membrane Fuel Cell using Sliding Mode

Junsheng Jiao
Department of Electronic Engineering, Tongling University, Tongling city Anhui province China, 244061
Corresponding author, e-mail: jiaotlu@sina.com

Abstract
Due to the nonlinear P-I characteristic of fuel cells, it is very important to implement a maximum power point tracking (MPPT) controller for practical applications. Based on analyzing the output characteristics of fuel cell power system, this paper presents extremum seeking sliding mode control method for MPPT of fuel cell power system under variable temperature and water content conditions. The approach is a combination of the extremum seeking and sliding mode methods. The simulation results show that the approach improves clearly the tracking efficiency of the maximum power available at the output of the fuel cell modules. The new method reduces the oscillations around the MPP, which has shown better performances.

Keywords: fuel cell, MPPT, slidng mode, extremum seeking

1. Introduction

Fuel cells are electro-chemical devices that directly convert chemical energy into electricity. Fuel cells have been attracting a great deal of interest in recent years because of their advantages such as high energy efficiency and clean operations. With these advantages, fuel cells are expected to solve several major challenges in the globe, including shortage of petroleum, air pollution, and global warming.
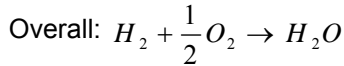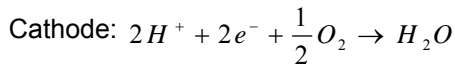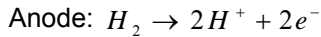
There are different types of fuel cells currently under development, including Proton Exchange Membrane Fuel Cell (PEMFC), Molten Carbonate Fuel Cell (MCFC) and Solid Oxide Fuel Cell (SOFC). Each type of fuel cell has its own advantages, limitations, and applications. In this work, we focus on the Proton Exchange Membrane Fuel Cell (PEMFC), also known as Polymer Electrolyte Membrane Fuel Cell. PEMFC employ a solid proton exchange membrane (PEM). The most important advantages are fast start-up compared with other fuel cell types [1]. However, the potential that affects their commercialization is cost for the fuel cell system. The life of fuel cell needs to be extended and cost needs to be reduced. The ability to increase the operation efficiency is a crucial issue for the design of fuel cell power system.

A lot of parameters can impact on produced power of PEMFC, but in any condition, there is one unique operating point on P-I curve which represents maximum power point (MPP) [2]. Several publications tackle the problem concerning the search of the optimal operating point by using various maximum power point tracking (MPPT) methods in order to extract the maximum energy from the photovoltaic power modules. The majority of these methods are based on so-called "perturbation and observation (P&O)" algorithms [3-4]. However, they display oscillatory behaviour around the MPP under normal operating conditions. Moreover, they can lead to a bad direction of the MPP tracking (i.e. towards less efficiency) in the case of a sudden variation of conditions when the system is already very near its actual MPP [5]. This is because the perturbation and observation (P&O) algorithm interprets the perturbation as the result of its previous variation of operating voltage, and expects its next variation to be in the same direction as that of the previous one.

This paper developed in tracking the fuel cell maximum power point by using sliding mode extremum seeking algorithm. The technique is attractive and provides the fastest speed of convergence towards the MPPT.

2. Static Model of PEMFC

PEM fuel cells consist of three major components-an anode, typically featuring a platinum or platinum-containing catalyst, a thin, solid polymeric sheet which acts as electrolyte, and a cathode, also platinum-catalysed. The various reactions for a PEM fuel cell fed with a hydrogen-containing anode gas and an oxygen-containing cathode gas, are [6]:

Anode: $H_2 \rightarrow 2H^+ + 2e^-$

Cathode: $2H^+ + 2e^- + \frac{1}{2}O_2 \rightarrow H_2O$

Overall: $H_2 + \frac{1}{2}O_2 \rightarrow H_2O$

The products of this process are DC electricity, liquid water and heat. The output voltage of a single cell can be defined as reversible voltage E_{nerst}, activation loss V_{act}, ohmic loss V_{ohmic} and concentration loss V_{con}. The basic expression for the voltage for a single cell is:

$$V_{FC} = E_{nernst} + V_{act} + V_{ohmic} + V_{con} \tag{1}$$

Where E_{nerst} is the thermodynamic potential of the cell and it represents its reversible voltage; V_{act} is known as activation overpotential voltage drop due to the activation of the anode and cathode; V_{ohm} is a measure of ohmic voltage drop; V_{con} represents the voltage drop resulting from the concentration or mass transportation of the reacting gases.

E_{nerst} is described by the Nernst equation. The expression is the Nernst equation for the hydrogen oxygen fuel cell, using literature values for the standard-state entropy change, can be written [7]:

$$E_{nernst} = 1.229 - 8.5 \times 10^{-4}(T - 298.15) + 4.31 \times 10^{-5}T \times (\ln P_{H_2} + 0.5 \ln P_{O_2}) \tag{2}$$

Where T is the cell operating temperature (K); P_{H2} and P_{O2} represent the partial pressures of hydrogen and oxygen (atm), respectively.

V_{act} is described by the Tafel equation, which can be expressed as [8]:

$$V_{act} = \xi_1 + \xi_2 T + \xi_3 T \ln C_{O_2} + \xi_4 T \ln I_{FC} \tag{3}$$

Where I_{FC} is the static current passing through the cell and ξ_{1-4} represents the experimental coefficients depending on each type of cell. Oxygen concentration in the interface between the cathode and the catalyst (mol/cm³) is given by:

$$C_{O_2} = \frac{P_{O_2}}{5.08 \times 10^6 \times e^{\frac{-498}{T}}} \tag{4}$$

V_{ohmic} results from the resistance of the polymer membrane in electron and proton transfers. It can be expressed as:

$$V_{ohmic} = -I_{FC}R_m \tag{5}$$

The ohmic resistance R_m is given by:

$$R_m = \frac{\rho_m l_m}{A} \tag{6}$$

Where ρ_m is membrane resistivity (Ω.cm)to proton conductivity; l_m is membrane thickness (cm); A cell active area (cm²). Membrane resistivity depends strongly on membrane humidity and temperature, For Nafion membranes, the specific resistivity is given as [8-9]:

$$\rho_m = \frac{181.6\left[1 + 0.03\frac{I_{FC}}{A} + 0.0062(\frac{T}{303})^2(\frac{I_{FC}}{A})^{2.5}\right]}{\left[y - 0.634 - 3(I_{FC}/A)\right]e^{4.18(1-303/T)}} \tag{7}$$

The water content y is an adjustable parameter with a maximum value of 23. This parameter depends on the membrane fabrication process and is a function of the relative humidity and the stoichiometric rate of the gas in the anode. Under ideal humidity conditions (100%), this parameter may have a value ranging from 14 to 20.

V_{con} represents the voltage drop resulting from the concentration or mass transportation of the reacting gases. The equation for concentration overvoltage is shown by:

$$V_{con} = B(1 - \frac{I_{FC}}{I_{L\max}A}) \tag{8}$$

Where I_{Lmax} is the limiting current. It denotes the maximum rate at which a reactant can be supplied to an electrode. In this paper, the model Ballard Mark V is adopted and the parameters are listed in Table 1 [10].

Table 1. Model Parameters

Parameter	Value	Parameter	Value
ξ_1	-0.948	P_{O2}(atm)	1
ξ_2	0.00354	P_{H2}(atm)	1
ξ_3	7.6×10^{-5}	T(K)	343
ξ_4	-1.93×10^{-4}	B(V)	0.016
l_m (μm)	178	I_{Lmax}(mA/cm^2)	1500
A(cm^2)	50.6	P_{max}(W)	19

3. Extremum Seeking Algorithm

Extremum seeking control (ESC) method developed in tracking MPP by R. Leyva [11], the stability of the Extremum Seeking algorithm was proved. As can be seen in Figure 1, the equations describing the system behaviour are composed by an integrator.
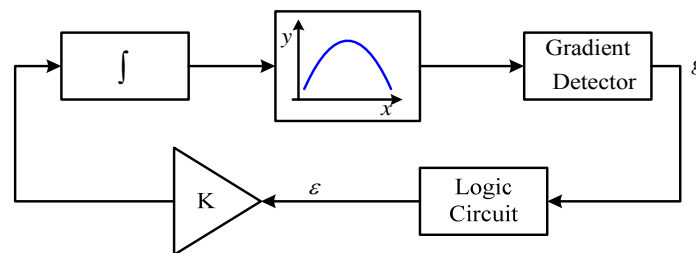

Figure 1. A Block Diagram of ESC Control System

$$\frac{dx}{dt} = K\varepsilon \tag{9}$$

where ε = ±1 and K is a positive constant, a differentiator:

$$g = \frac{dy}{dt} \tag{10}$$

A logic circuitry subsystem is associated and implemented according to the following function:

If g<0, then the sign of ε must change.
If g>0, then the sign of ε keeps the same.
Figure 2 explains the behaviour of the ESC algorithm. Four cases can be distinguished. Marked in Figure 2 are the variations in dx/dt and dy/dt of the four points a, b, c, d:

$$a : (\frac{dx}{dt})\Big|_{t=t^-} > 0, \ (\frac{dy}{dt})\Big|_{t=t^-} > 0 \Rightarrow (\frac{dx}{dt})\Big|_{t=t^+} = k$$

$$b : (\frac{dx}{dt})\Big|_{t=t^-} > 0, \ (\frac{dy}{dt})\Big|_{t=t^-} < 0 \Rightarrow (\frac{dx}{dt})\Big|_{t=t^+} = -k$$

$$c : (\frac{dx}{dt})\Big|_{t=t^-} < 0, \ (\frac{dy}{dt})\Big|_{t=t^-} > 0 \Rightarrow (\frac{dx}{dt})\Big|_{t=t^+} = -k$$ (11)

$$d : (\frac{dx}{dt})\Big|_{t=t^-} < 0, \ (\frac{dy}{dt})\Big|_{t=t^-} < 0 \Rightarrow (\frac{dx}{dt})\Big|_{t=t^+} = k$$

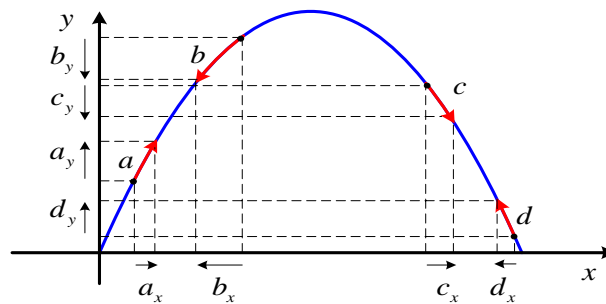Where:

$$\frac{dy}{dx} = \frac{dy}{dt}\frac{dx}{dt}$$ (12)

Figure 2. Illustrative Cases of Extremum Seeking

It can be expressed as the follows. Since dy/dx=(dy/dt)(dx/dt), the above four cases can be expressed in compact form as follows:

$$\text{If } (\frac{dy}{dx})\Big|_{t=t^-} > 0 \text{ then } (\frac{dx}{dt})\Big|_{t=t^+} = k$$ (13)

$$\text{If } (\frac{dy}{dx})\Big|_{t=t^-} < 0 \text{ then } (\frac{dx}{dt})\Big|_{t=t^+} = -k$$ (14)

Equation (13) and (14) can also be reduced to only one expression

$$\frac{dx}{dt} = K sign(\frac{dy}{dx})$$ (15)

It can be notice that the algorithm evaluates the sign of dy/dt, whereas the resulting dynamics are dependent of dy/dx. Also, it can be observed in Equation (15) that the equilibrium point dx/dt =0 corresponds to an extremum of the x-y curve in Figure.2, where dy/dx =O. In order to demonstrate that the equilibrium point is stable, a positive function V(t) is defined in a concave domain of y(x).

$$V_{L_y}(t) = \frac{1}{2}(\frac{dy}{dx})^2 \tag{16}$$

The first time derivative of Equation (16) yields:

$$\dot{V}_{L_y}(t) = \frac{dy}{dx}\frac{d^2y}{dx^2}\left[Ksign(\frac{dy}{dx})\right] \tag{17}$$

The concavity of y(x) can be translated by Equation (13) and (14):

$$\frac{d^2y}{dx^2} < 0 \tag{18}$$

$$\frac{dy}{dx}sign(\frac{dy}{dx}) > 0 \tag{19}$$

Hence, a choice of positive K satisfies $\dot{V}_{L_y}(t) < 0$, i.e. , a validated stability.

As the P-I characteristics of fuel cell is a concave function, the previous analysis can be applied to MPPT controllers.

4. Sliding Mode ESC

Sliding Mode ESC block diagram has been depicted in Figure 3. The main advantage of this ESC algorithm is that it does not require gradient sensors. A sliding surface is defined as:
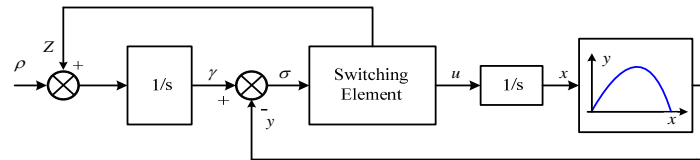
$$\sigma = \gamma - y \tag{20}$$

Figure 3. A Block Diagram of a Sliding Mode ESC System.

In Figure 3, it is known that:

$$u = dx / dt \tag{21}$$

$$u = U_0 sign(\sigma) \tag{22}$$

$$dr / dt = \rho + Z \tag{23}$$

$$Z = -Z_0 sign(\sigma) \tag{24}$$

Where U_0, Z_0 , ρ: positive constant;
u, Z: switching elements to drive x and y toward optimal value respectively;
r: optimal track of the output power;
σ: the given acceleration of r.

According to Equation (20)

$$\frac{d\sigma}{dt} = \rho - Z_0 \cdot sign(\sigma) - dy / dx \cdot U_0 \cdot sign(\sigma) \tag{25}$$

The function sign (σ) is defined as:

$$sign(\sigma) = \begin{cases} 1 & \text{for } \sigma > 0 \\ 0 & \text{for } \sigma = 0 \\ -1 & \text{for } \sigma < 0 \end{cases} \tag{26}$$

When the sign of derivative of ε changes then a sliding mode motion occurs, and x is steered towards optimal value while y tracks r. The required parameters to set up the sliding mode ESC algorithm are U_0, Z_0, ρ. The following relationships must hold.

$$\begin{cases} Z_0 >> U_0 \\ Z_0 >> \rho \end{cases} \tag{27}$$

In order to prove the stability of above sliding mode ESC scheme, the Lyapunov function is selected as:

$$V(t) = \frac{1}{2}\sigma^2 \tag{28}$$

Then its first derivative with respect to time is:

$$\begin{aligned} \dot{V}(t) = \sigma\dot{\sigma} &= \sigma\left[\rho - Z_0 sign(\sigma) - U_0 \frac{dy}{dx} sign(\sigma)\right] \\ &= \sigma\rho - Z_0|\sigma| - U_0 \frac{dy}{dx}|\sigma| \\ &\leq \left[\rho - Z_0 - U_0 \frac{dy}{dx}\right]|\sigma| \end{aligned} \tag{29}$$

In the neighborhood of MPPT, the value of dy/dx tends to zero, and it is assumed that $Z_0 >> \rho$ and $Z_0 >> U_0$. Therefore, a chance of suitable positive Z_0 satisfies:

$$\dot{V}(t) < 0 \tag{30}$$

Thus, we can see that the designed MPPT algorithm based on sliding mode ESC for PEMFC power system does not require gradient sensors. The control system can enter swiftly the sliding surface and reach the robust conditions.

5. Simulation Result

To verify the proposed method, the MPPT procedure is implemented in Matlab/Simulink as illustrated in Figure 4. Thirty is the number of the series-wound fuel cells in the stack. In the simulation, the values of Z_0, U_0, and ρ are set as 9000, 200 and 150 respectively. Simulation parameters of the model are indicated in Table 1.
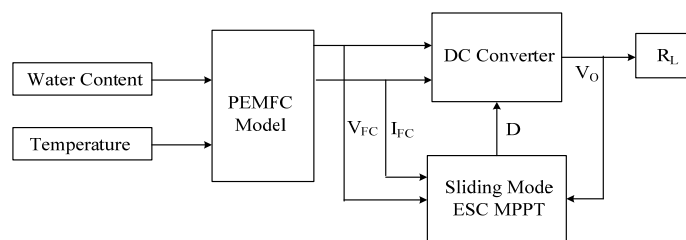

Figure 4. MPPT Control Block Diagram

The MPPT algorithm is used to control the output power in fuel cell stack. In Figure 5, simulation has been performed when fuel cell temperature changes with a transient process of about 0.01-0.02s, which cause the P-I curves of fuel cell stack to change. The proposed method can track the maximum power by adjusting the voltage. As fuel cell temperature declining from 380K to 340K at time=0.15s, the output power rapidly descends and then tends to the maximum one. It can also provide a power generation system to quickly generate the maximum power corresponding to condition change.
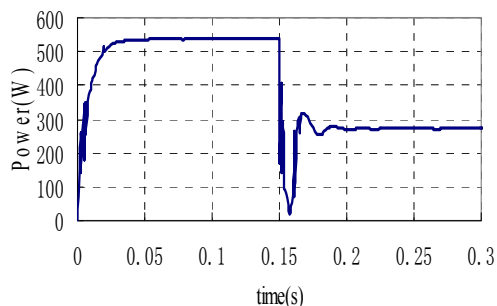

Figure 5. Responses of System Output with Temperature Change from 380K to 340K at time=0.15s
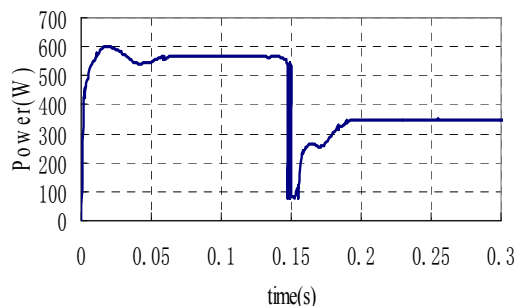

Figure 6. Responses of system output with water content change from 16 to 7 at time=0.15s

It can be further noticed that responses of system output change in water content. The MPPT is achieved along with tracking the maximum power point of fuel cell. Figure 6 illustrates the tracking result with step water content input (from 16 to7) under the same temperature. The system reaches maximum power within 0.01s. Thus, a desirable performance of fuel cell power system is observed for the MPPT.

6. Conclusion

In this paper, a sliding mode ESC approach has been introduced for the maximum power tracking of PEMFC power generation systems. Even considering uncertainties, the controlled system assures finite time convergence of MPP tracking. Through simulations, this new approach shows that the tracking efficiency of the MPP is better than that obtained with the classic P&O method. The new nonlinear method produced practically no oscillations around the MPP, which is the main weakness of the P&O method. Therefore, the control method assures better tracking performance.

References
[1] J Pukrushpan, A Stefanopoulou, H Peng. Control of Fuel Cell Breathing. *IEEE Control System*. 2004; 24(2): 30-46.
[2] Koutroulis E, Kalaitzakis K, Voulgaris NC. Development of a Microcontroller based Photovoltaic Maximum Power Point Tracking Control System. *IEEE Trans Power Electron*. 2001; 16(1): 46-54.
[3] D. Sera, R. Teodorescu, J. Hantschel and M. Knoll. Optimized Maximum Power Point Tracker for Fast-Changing Environmental Conditions. *IEEE Transaction on Industrial Electronics*. 2008; 55(7): 2629-2637.
[4] Hua C, Lin J, Shen C. Implementation of a DSP-controlled Photovoltaic System with Peak Power Tracking. *IEEE Transaction on Industrial Electronics*. 1998; 45(2): 99-107.
[5] Chiang J, Chang KT, Yen CY. Residential Photovoltaic Energy Storage System. *IEEE Transaction on Industrial Electronics*. 1998; 45(3): 385-394.
[6] JC Amphlett, RF Mann, BA Peppley, PR Roberge, A Rodrigues. A Model Predicting Transient Responses of Proton Exchange Membrane Fuel Cell. *Journal of Power Sources*. 1996; 61(1): 183-188.
[7] Marcos V Moreiraa, Gisele E da Silva. A Practical Model for Evaluating the Performance of Proton Exchange Membrane Fuel Cells. *Renewable Energy*. 2009; 34(7): 1734-1741.

[8] Xingguan Ma, Jiao Wang, Xiangxin Xue, Yulan Tang, Jinxiang Fu. Simulation Biomass Effecting On Microbial Fuel Cell Electricity Properties and Substrate Degradation. *TELKOMNIKA Indonesia Journal of Electrical Engineering*. 2013; 11(2): 559-566.

[9] Doaa M Atia, Faten H Fahmy, Ninet M Ahmed, Hassen T Dorrah. A New Control and Design of PEM Fuel Cell System Powered Diffused Air Aeration System. *TELKOMNIKA Indonesia Journal of Electrical Engineering*. 2012; 10(2): 291-302.

[10] JM Correa, FA Farret, LN Canha, Marcelo G Simoes. An Electrochemical-Based Fuel-Cell Model Suitable for Electrical Engineering Automation Approach. *IEEE Transactions on Industrial Electronics*. 2004; 51(5): 1103-1112.

[11] R Leyva, C Alonso, A Cid-Pastor. MPPT of Photovoltaic System using Extremum-Seeking Control. *IEEE Aerospace and Electronic Systems*. 2006; 42(1): 249-258.